Available online at www.sciencedirect.com

SCIENCE DIRECT®

Environmental Pollution 137 (2005) 295–304

ENVIRONMENTAL POLLUTION

www.elsevier.com/locate/envpol

Acid neutralization within limestone sand reactors receiving coal mine drainage

Barnaby J. Watten[a,*], Philip L. Sibrell[a], Michael F. Schwartz[b,1]

[a]United States Geological Survey, Leetown Science Center, 11649 Leetown Road, Kearneysville, WV 25430, USA
[b]The Conservation Fund - Freshwater Institute, 1098 Turner Road, Shepherdstown, WV 25443, USA

Received 17 September 2004; accepted 28 January 2005

A new treatment method for acid mine drainage is described.

Abstract

Pulsed bed treatment of acid mine drainage (AMD) uses CO_2 to accelerate limestone dissolution and intermittent fluidization to abrade and carry away metal hydrolysis products. Tests conducted with a prototype of 60 L/min capacity showed effective removal of H^+ acidity over the range 196–584 mg/L ($CaCO_3$) while concurrently generating surplus acid neutralization capacity. Effluent alkalinity (mg/L $CaCO_3$) rose with increases in CO_2 (DC, mg/L) according to the model Alkalinity = 31.22 + 2.97(DC)$^{0.5}$, where DC was varied from 11–726 mg/L. Altering fluidization and contraction periods from 30 s/30 s to 10 s/50 s did not influence alkalinity but did increase energy dissipation and bed expansion ratios. Field trials with three AMD sources demonstrated the process is capable of raising AMD pH above that required for hydrolysis and precipitation of Fe^{3+} and Al^{3+} but not Fe^{2+} and Mn^{2+}. Numerical modeling showed CO_2 requirements are reduced as AMD acidity increases and when DC is recycled from system effluent.

Keywords: Acid mine drainage; Treatment; Fluidized bed; Limestone; Carbon dioxide

1. Introduction

Mining processes resulting in acid deposition have had a significant negative effect on aquatic resources in North America, as well as many other parts of the world, including the loss of important fisheries (Maree et al., 1996; Starnes and Gasper, 1995; Cole et al., 2001a,b). Acid mine drainage (AMD) results primarily from the dissolution of the metallic sulfide FeS_2, and its subsequent oxidation to sulfuric acid (Evangelou, 1995). This reaction is followed by the hydrolysis of the product Fe^{3+} to the insoluble product ferric hydroxide ($Fe(OH)_3$). Acid generated here and in the first oxidation step forces the solubilization of certain base metals, including Al^{3+} and Mn^{2+}, that contribute acidity as well as additional solids while undergoing alternate hydrolysis reactions (Evangelou, 1995; Hedin et al., 1994).

Mitigation of AMD is achieved through application of an acid-neutralizing reagent followed by gravity separation of the solid reaction products (Skousen et al., 1995; Maree and du Plessis, 1994). Reagent costs, clarifier retention time and sludge yield are minimized when $CaCO_3$ (limestone) is used as the alkaline reagent (Hedin et al., 1994; Dempsey and Jeon, 2001; Sibrell and Watten, 2003). Limestone use, however, is severely restricted by the development of Al^{3+}, Fe^{3+}, Mn^{2+}, and SO_4^{2-} based scales that restrict transport of reactants and products to

* Corresponding author. Tel.: +1 304 724 4425; fax: +1 304 724 4428.
E-mail addresses: barnaby_watten@usgs.gov (B.J. Watten), philip_sibrell@usgs.gov (P.L. Sibrell), m.schwartz@freshwaterinstitute.org (M.F. Schwartz).
[1] Tel.: +1 304 876 2815; fax: +1 304 870 2208.

0269-7491
doi:10.1016/j.envpol.2005.01.026

and from reactive surfaces (Lovell, 1973; Pearson and McDonnell, 1975a; Ziemkiewicz et al., 1997). Fixed beds of limestone are also prone to the accumulation of solid reaction products within interstitial voids reducing hydraulic conductivity as well as effective surface areas (Pearson and McDonnell, 1975b). Watten (1999) developed a pulsed limestone bed (PLB) process to accelerate limestone dissolution rates and to prevent the accumulation of solids. Water is directed intermittently through nozzles into limestone sand reactors establishing a repeating cycle of fluidization, bed turnover and contraction. Abrasion of scale from limestone surfaces is provided by collision forces generated hydraulically during bed expansion circumventing the need for high-torque drive components associated with rotating drum reactors (Lovell, 1973; Zurbuch, 1963). Further, the PLB process uses dissolved carbon dioxide (DC) to accelerate limestone dissolution by forcing the reaction of $CaCO_3$ with CO_2 to form the product bicarbonate

$$CaCO_3 + CO_2 + H_2O \leftrightarrow Ca^{2+} + 2HCO_3^- \quad (1)$$

and by increasing the acidity of the AMD within the reactor so as to sustain the reaction of H^+ with $CaCO_3$, i.e.,

$$CO_2 + H_2O \leftrightarrow H_2CO_3 \leftrightarrow H^+ + HCO_3^- \quad (2)$$

$$CaCO_3 + H^+ \leftrightarrow HCO_3^- + Ca^{2+} \quad (3)$$

Sverdrup (1985) developed an overall dissolution rate expression for $CaCO_3$ that includes the effect of Reactions (1) and (3):

$$-\frac{dm}{dt} = \left[k_1[H^+] + k_2[CO_2] + k_w - k_b\left([Ca^{++}]\left[HCO_3^-\right]\right)\right] \times \left(\frac{3m}{\rho r}\right) \quad (4)$$

where [ ] refers to the bulk solution concentration, k_1 and k_2 are first-order reaction constants, k_w is a zero order constant for the reaction of $CaCO_3$ with H_2O, k_b is a constant for the backward reaction driven by the interaction of Ca^{2+} and HCO_3^- with $CaCO_3$, m is mass of particle, ρ is the density of the limestone and r is particle radius. Reaction (3), represented by the product $k_1[H^+]$, decreases with increasing pH but remains the primary mechanism of limestone dissolution up to a pH of about 4.7 (Plummer et al., 1978). At pH > 4.7, limestone dissolution can be accelerated by increasing DC so as to exploit Reaction (1), represented here by the product $k_2[CO_2]$ (Plummer et al., 1978; Watten et al., 2004a). High DC levels also elevate equilibrium concentrations of HCO_3^- (Stumm and Morgan, 1996) and thereby allow for surplus acid neutralization capacity (alkalinity) in the reactor's effluent (Hedin et al., 1994; Mitchell and Wildeman, 1996). DC not reacted away is stripped from the effluent then reused to minimize make-up CO_2 requirements (Watten, 1999; Sibrell et al., 2000). Decarbonation of the effluent reduces acidity providing a desirable upward shift in equilibrium pH (Pearson et al., 1982).

Watten et al. (2004a) correlated PLB limestone dissolution rates with reactor pressure (P_{CO_2}, range 0–690 kPa), inlet acidity (Acy, range 6–1033 mg/L) and reactor bed height (H). Sulfuric acid acidity was neutralized while generating high concentrations of alkalinity (36–1086 mg/L) despite a hydraulic residence time of just 4.2–5.0 min. Alkalinity (mg/L $CaCO_3$) rose with increases in influent acidity and P_{CO_2} according to the model:

$$\text{Alkalinity} = a + b(P_{CO_2})^{0.5} + c(\text{Acy}) - d(P_{CO_2})^{0.5}(\text{Acy})$$

where a, b, c, and d are regression coefficients. Alkalinity decreased at an increasing rate with reductions in H from 77.5 to 27.3 cm. Using similar methods, Lee (2003) evaluated the effects of hydraulic residence time (HRT) and temperature on PLB performance. Alkalinity increased linearly with HRT (HRT range 6–15 min). Temperature effects on alkalinity were minor – with P_{CO_2} = 209 kPa, alkalinity decreased from 900 mg/L at 12 °C to 800 mg/L at 22 °C. Pilot scale field tests of the PLB process (Hammarstrom et al., 2003; Sibrell and Watten, 2003; Sibrell et al., 2000, 2003), have demonstrated effective treatment of AMD containing unusually high concentrations of acidity (1096 mg/L), and iron (200 mg/L) as well as the potential for side-stream treatment with blending.

PLB reactors have used positive gage pressures to increase the saturation concentration of DC and hence the potential for CO_2 dosing (Colt, 1984). Further, the reactors have been linked, in a closed loop, to a carbonator that maintains target DC concentrations during treatment despite conversion of CO_2 to reaction products. In the present study, we evaluate performance of PLB reactors designed to operate at atmospheric pressure without water recirculation so as to reduce system complexity and perhaps allow un-attended operation in remote field applications. Specifically, we test the effects of intermittent fluidization (pulsing sequence), hydraulic loading rate and CO_2 dosing on effluent alkalinity. Further, we follow changes in water chemistry across the system when treating AMD from four different field sites both with and without CO_2 pretreatment.

2. Materials and methods

2.1. Test Series I – laboratory trials

Two replicate PLB systems were constructed each capable of processing 60 L/min. Fig. 1 shows the system's

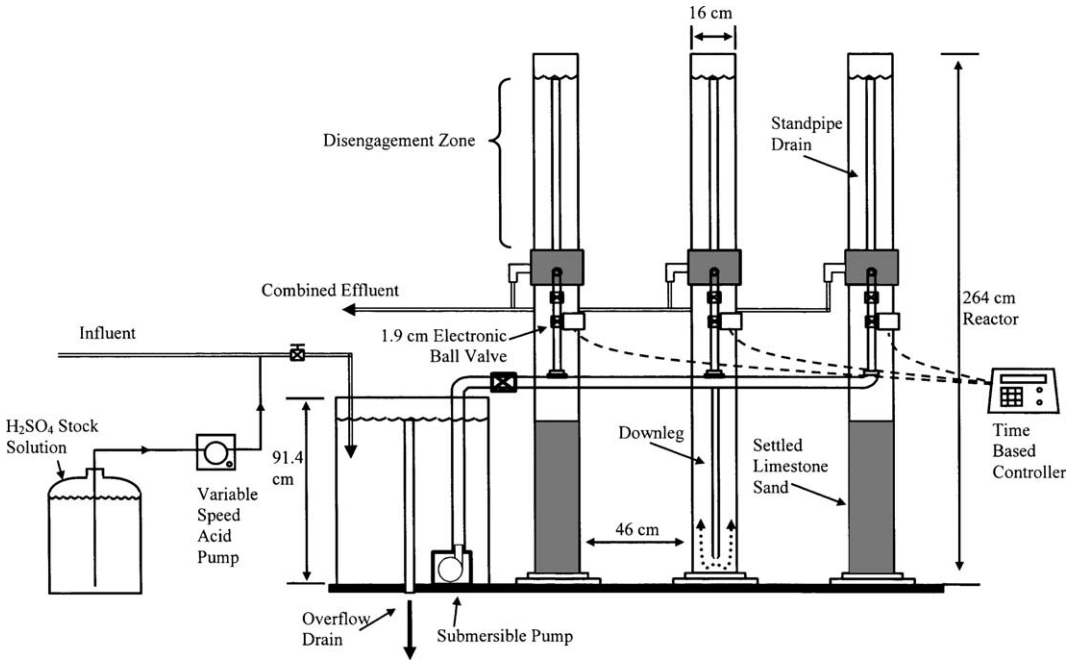

Fig. 1. Elevation view of the test system used to evaluate performance of intermittently fluidized beds of limestone sand. The center column is shown without limestone to illustrate the position of the down leg used to distribute influent AMD.

major components – three 16 cm diameter × 264 cm vertical reaction columns (clear plastic) charged with granular limestone, a 3.8 cm diameter feed solution manifold, a time-based electronic control system (Chron-Trol Corp., San Diego, CA, USA) used to direct the system's electrically actuated ball valves (Electromni ASAHI, Malden, MA, USA), a 0.25 m^3 feed solution sump and a 1.4 kW submersible pump (Goulds Pumps, Inc., Seneca Falls, NY, USA). Test systems were plumbed so that a single sump/pump could support, if needed, both replicate systems. Reaction columns were each charged with 18 kg of limestone sand rinsed prior to use with well water ($T = 9$ °C) at a hydraulic loading rate of 1240 L/m^2/min for 45 min. Settled bed heights ranged between 52 and 53 cm. The limestone sand used (Bell Mine Glass Stone #1, Bellefonte Lime Co., Bellefonte, Pa, USA) was 96.9% $CaCO_3$, had an effective size (D_{10}) of 159 μm, and a uniformity coefficient (D_{60}/D_{10}) of 3.3. Bed expansion and contraction was achieved by directing flow intermittently through a 1.3 cm diameter orifice positioned at the base of each column. Reactor effluent spilled into a standpipe fixed at the top of each column then was shunted into a drain manifold or released independently depending on test conditions. Feed solutions were acidified by mixing reagent grade sulfuric acid with well water at a rate fixed by the speed of a peristaltic pump (Barnant Co., Barrington, IL, USA). Feed solution DC was increased, when required, by directing well water through a packed tower type carbonator (Watten, 1999) receiving a regulated flow of CO_2 from a compressed gas cylinder or Dewar-type storage tank.

Effects of CO_2 pretreatment on system performance were evaluated by establishing reactor feed DC concentrations of 11, 109, 205, 447, and 726 mg/L at a common hydraulic loading (228 L/m^2/min). Valve timing maintained a repeating cycle of fluidization and contraction with durations of 20 s and 40 s, respectively. Three test columns were operated in parallel with effluents combined to provide a single discharge. Two observations were made under each set of test conditions. Valve timing effects on performance were evaluated in a separate test by establishing fluidization and contraction durations of 10 s/50 s, 20 s/40 s and 30 s/30 s. Hydraulic loading (average) was fixed at 373 L/m^2/min. Here three columns were operated independently during trials with each of the three test timing sequences. Feed solution DC was not elevated above normal well water concentrations (11 mg/L) but acidity was increased to 200 mg/L. This same acidity level was used to evaluate the effects of hydraulic loading on the performance of three columns operated independently as conventional fluidized beds, i.e., without pulsing. Observations here were made at a hydraulic loading rate of 571, 766 and 896 L/m^2/min. We then compared the performance of five columns operated independently in both the fixed flow and intermittent fluidization modes (20 s fluidization, 40 s contraction). In all cases hydraulic loading was 676 L/m^2/min with an inlet acidity of about 550 mg/L. DC was not elevated in this test, but DC was elevated in a second comparison of columns operating with and without intermittent fluidization. In this case DC was maintained at ambient, 418 and

572 mg/L. At each test DC level, one of two test columns was operated intermittently with fluidization and contraction periods of 20 s and 40 s, respectively, while the second column, operated in parallel, received flow continuously. The feed solution was AMD (Antrim Mine, Tioga County, PA, USA) trucked to our laboratory then introduced at a common hydraulic loading rate of 622 L/m^2/min. The temperature and acidity of the drainage was 12.8 °C and 340 mg/L. Two observations were made under each set of test conditions.

Treatment effect in all tests was established by comparing influent with effluent chemistry. Effluent samples were composites taken at a fixed rate during a complete treatment cycle. Analyses followed APHA (1995) and included temperature, pH, alkalinity, DC and acidity. Water flow rate was determined by measuring time required to fill a container of known volume. Hydraulic residence time was calculated as the total reactor volume, minus limestone volume, divided by influent flow rate. Hydraulic loading rate was calculated as the average total reactor flow rate divided by the total cross-sectional area of the columns in use.

2.2. Test Series II – field trials

Field tests of the PLB prototype were completed in cooperation with the Pennsylvania Department of Environmental Protection at the Toby Creek AMD Treatment Plant, Dagus Mines, PA, USA. AMD from Portal A, located immediately adjacent to the treatment plant, was pumped concurrently through each of the six columns. Three were operated with a carbonation pretreatment step (inlet $P_{CO_2}=135$ mmHg) and three were operated without pretreatment (inlet $P_{CO_2}=9$ mmHg). All columns were evaluated at a hydraulic loading rate of 300–320 L/m^2/min. Influent and effluent samples (three per treatment) were taken over the course of a 7.6 h test period. A second test established process performance when treating AMD trucked to the plant from each of the two additional sources identified here as Brandy Camp and Kyler Run. In both cases, influent and effluent samples (three) were obtained from single columns (no CO_2 addition) operating over a test period of about 6 h. Here the hydraulic loading rate was held within the range 330–340 L/m^2/min. Single columns were used to minimize AMD trucking requirements. Fluidization and contraction periods in all tests were 60 s and 120 s, respectively. Settled bed heights ranged between 66 and 80 cm. Limestone was replaced in the test columns after completion of each AMD source specific test series. Prototype performance was assessed as in Test Series I except influent and effluent chemistry analyses were performed by the PA Department of Environmental Protection, Harrisburg PA. Analyses were based on EPA (1983) methods and included pH, alkalinity, hardness, Ca^{2+}, Fe (total iron), Fe^{2+}, Mn^{2+}, Al^{3+}, and acidity (hot peroxide treatment). Effluent samples were analyzed following a 7 min air-stripping step both with and without subsequent filtering through a glass fiber filter (1.5 μm pore size). Metal removals were calculated based on differences in concentration between the influent and filtered effluent samples. Influent temperature and dissolved oxygen were measured with a polarographic oxygen meter (Yellow Springs Instrument Co., Yellow Springs, OH, USA). Influent CO_2 tension (mmHg) was determined with a headspace analyzer (Watten et al., 2004b) coupled with an infrared CO_2 gas phase meter (CEA Instruments, Emerson, NJ, USA). Local barometric pressure was measured with a pressure transducer (Solomat Partners Ltd, Stamford, CT, USA).

Statistical analyses supporting all tests were completed using either Sigma Stat (version 2.0) or Table Curve 2D (version 5.0) software. Specific analyses included Student's *t*, one-way ANOVA, two-way repeated measures ANOVA, linear regression, Tukey's test and the Mann–Whitney rank sum test.

3. Results

3.1. Test Series I – laboratory trials

Fig. 2 shows the effects of CO_2 addition on effluent alkalinity when operating with a timing sequence of 20 s/40 s (fluidization/contraction) and a hydraulic loading rate of 228 L/m^2/min (HRT = 9.8 min). Effluent alkalinity increased to a high of 114.4 mg/L with increases in DC following the model:

$$\text{Alkalinity} = 31.217 + 2.972(\text{DC})^{0.5}$$
$$R^2 = 0.985;\ P < 0.001;\ \text{DF} = 9;\ F = 515.27 \qquad (5)$$

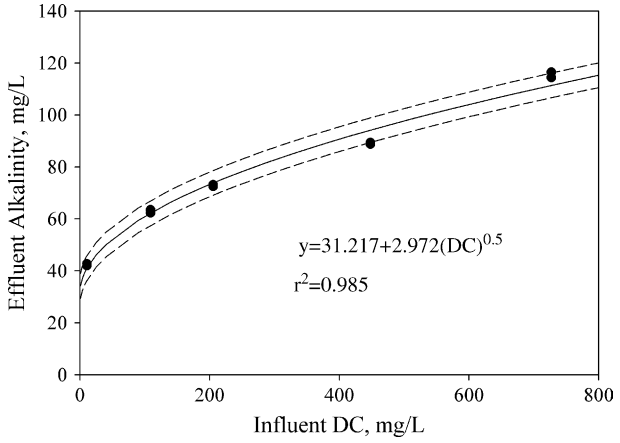

Fig. 2. Effect of influent CO_2 concentration (DC) on effluent alkalinity (Test Series I).

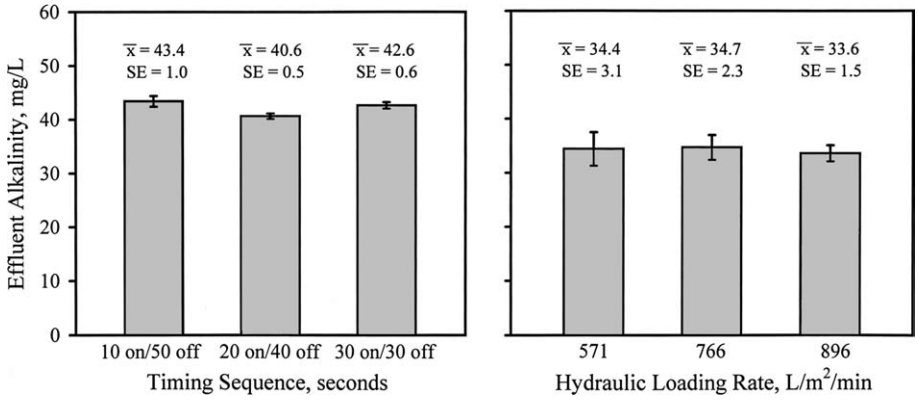

Fig. 3. Effects of reactor timing sequence and hydraulic loading rate on effluent alkalinity (Test Series I). Standard errors are listed as SE.

Fig. 3 shows the effects of timing sequence on effluent alkalinity when feed solution acidity was increased to a mean of 202 (SD 4.7) mg/L. Effluent alkalinity averaged 42.2 mg/L with a pH range of 5.85–6.09. Differences between alkalinity established with timing sequences of 10 s/50 s, 20 s/40 s, and 30 s/30 s (Fig. 3) were not statistically significant ($P > 0.05$). Expanded bed heights, as a percent of settled bed height, were correlated with timing sequence despite use of a common average hydraulic loading rate (HRT = 6.0 min):

$$\text{Bed Expansion (\%)} = 73.922 - (0.985(\text{sec fluidized}))$$
$$R^2 = 0.968;\ P < 0.001;\ \text{DF} = 8;\ F = 104.753 \qquad (6)$$

Also shown in Fig. 3 is the response of alkalinity to changes in hydraulic loading rate over the range 571–896 L/m^2/min when columns were operated in the fixed flow mode (HRT = 2.5–3.9 min). Here, inlet acidity was 196 (SD 2.0) mg/L. Effluent alkalinity averaged 34.2 (SD 3.63) mg/L and did not differ significantly among treatment groups ($P > 0.05$). Bed expansion ratios were 24, 64, and 100% for hydraulic loadings rates of 571, 766, and 896 L/m^2/min. Inlet acidity was increased to 584 (SD 26.1) mg/L during tests comparing performance of five columns operated in both the fixed flow and intermittent fluidization modes (HRT = 3.3 min). Effluent alkalinity established for columns operating with a timing sequence of 20 s/40 s averaged 48.4 (SD 1.74) mg/L and was significantly lower ($P < 0.001$) than the average established with a fixed flow (58.7 (SD 0.51) mg/L). Intermittent fluidization, however, provided expanded bed heights that were greater ($P < 0.001$) than bed heights maintained by the fixed flow operating mode – the mean bed expansion ratio was 105.1% with intermittent fluidization and 61.3% for the fixed flow case. While influent DC was not elevated in this test, it was in the second comparison of alkalinities (Table 1) established with intermittent and fixed flow rates (HRT = 3.6 min). Alkalinity ranged from 25.7 to 92.0 mg/L with inlet and effluent pH ranges of 2.96–3.02 and 5.23–5.58, respectively. Overall, DC had a positive significant effect ($P < 0.001$) on alkalinity but operating mode effects on this same variable were not significant ($P > 0.05$). A temperature increase of ≤ 1 °C was observed across the system under each of the test conditions evaluated.

3.2. Test Series II – field trials

Table 2 gives changes in water chemistry across the PLB system when treating Source A AMD with and without CO_2 pretreatment (HRT = 7.0–7.4 min). Influent temperature, dissolved oxygen and local barometric pressure ranges were 9.5–9.8 °C, 3.0–3.8 mg/L and 719–720 mmHg. Expanded bed heights represented 186–201% of settled bed heights. CO_2 pretreatment increased ($P < 0.01$) effluent pH and alkalinity from means of 6.5 to 6.9 and from 58.7 to 149.3 mg/L. Associated increases in Ca^{2+} with CO_2 addition were also significant ($P < 0.05$). However, CO_2 pretreatment did not affect ($P > 0.05$) Al, Fe, and Mn removals calculated based on influent and filtered effluent samples. The mean removal values here were: Al, 98.6%; Mn, 0.0%; Fe, 81.4%. Fe^{2+} removal was higher with CO_2 pretreatment than without ($P < 0.05$) – 35.1% versus 16.2%. Filtration did not ($P > 0.05$) influence effluent

Table 1
Comparison of pulsed and fixed flow rates on column effluent alkalinity (mg/L as $CaCO_3$) when treating antrim mine AMD

Test condition	Effluent alkalinity		Group mean ± SE
	Pulsed flow	Fixed flow	
No CO_2 addition	31.8 (0.4)	25.7 (2.6)	28.7 ± 0.52
CO_2 addition			
DC = 419 mg/L	58.5 (2.1)	63.5 (3.5)	61.0 ± 0.52
DC = 572 mg/L	*85.8* (3.2)	*92.0* (2.1)	88.9 ± 0.52
Group mean ± SE	58.7 ± 0.44	62.4 ± 0.44	

Values are means ($N = 2$) followed in parentheses by standard deviations.

Table 2
Effect of inlet P_{CO_2} on changes in water chemistry across the test system when treating source A AMD at Toby Creek

Variable	*I*	P_{CO_2} = 9 mmHg EF	P_{CO_2} = 135 mmHg EF
pH	3.2 (0.0)	6.5 (0.0)**	6.9 (0.1)**
Acidity, mg/L	215.3 (8.1)	0.0 (0.0)	0.0 (0.0)
Alkalinity, mg/L	0.0 (8.1)	58.7 (5.0)**	149.3 (6.1)**
Al, mg/L	14.8 (1.5)	0.2 (0.2)	0.2 (0.1)
Fe^{2+}, mg/L	3.7 (0.2)	3.1 (0.1)*	2.4 (0.4)*
Fe, mg/L	16.1 (1.0)	3.2 (0.1)	2.8 (0.2)
Mn, mg/L	6.0 (0.3)	6.2 (0.5)	5.8 (0.4)
Ca, mg/L	83.2 (5.3)	176.7 (14.5)*	217.1 (11.6)*

EF values marked with an asterisk are significantly different (*I* = influent mean; *N* = 3–6; EF = effluent filtered mean, *N* = 3).
*$P < 0.05$.
**$P < 0.01$.

alkalinity or Ca^{2+} concentrations indicating both variables were present primarily as dissolved solids.

Table 3 gives changes in water chemistry across the PLB system when treating AMD from Brandy Camp and Kyler Run (HRT = 6.6–6.8 min). Influent water temperature at both sites was similar ranging between 10.2 and 10.8 °C. DO averaged 3.6 mg/L in the Brandy Camp source and 5.7 mg/L in the Kyler Run source. Calculated Al^{3+} removal efficiencies, based on a comparison of influent versus filtered samples, were high in all tests ranging between 96.1 and 97.6%. However, corresponding Fe^{2+} and Mn removal efficiencies were low, averaging, respectively, 9.8% and 14.0% for Brandy Camp and 13.9% and 0.0% for Kyler Run. Iron was present in both AMD sources primarily as Fe^{2+} and so removal of Fe (total) was also low (7.0–16.8%). The low Fe^{2+} and Mn removal rates no doubt contributed to the residual acidities observed.

4. Discussion

4.1. Limestone dissolution

The PLB process was designed to circumvent armoring by iron and aluminum based precipitates by increasing limestone dissolution with elevated DC and by creating hydrodynamic conditions that keep particle surfaces clean of hydrolysis reaction products. Carbonation accelerates limestone dissolution by maintaining a higher mean H^+ concentration within the reactor (Eq. (2)) while forcing the reaction of $CaCO_3$ with CO_2 to form bicarbonate alkalinity (Eq. (1)). Fig. 2 shows alkalinity increased with DC concentration following the model $y = a + b(DC)^{0.5}$ over the DC range 11–726 mg/L. This model form agrees with that reported for the early PLB system configuration (Watten et al., 2004a), but model coefficients established in the present study were relatively low despite our 2.3-fold increase in HRT − 9.8 versus 4.2 min. Our regression-derived intercept and slope values were, respectively, 31.15 and 14.63 for the present study and 39.73 and 39.24 for the data set from Watten et al. (2004a) when DC is expressed as a partial pressure (P_{CO_2}, kPa) based on Colt (1984). Model use indicates effluent alkalinity will represent about 58% of that predicted for the early PLB configuration when operating at the same P_{CO_2}. The reduced sensitivity to P_{CO_2} observed is probably related to our use of a PLB configuration that did not include an internal recirculation loop. The latter provides for a more uniform level of DC throughout the treatment cycle despite conversion of CO_2 to bicarbonate (Eq. (1)), but requires additional valving and energy input.

Fig. 4 compares the effluent alkalinity observed (line A) with that predicted (9 °C) at equilibrium (lines B, C, D) using geochemical modeling software (Parkhurst, 1995). All data show a dependence on DC although PLB data are well below the equilibrium concentrations shown. Line B, for example, gives the predicted saturation concentration of alkalinity that corresponds to specific DC concentrations when CO_2 is not limited to the initial charge provided by pretreatment, i.e., when a recirculation loop is used that includes a carbonator designed to maintain a target level of DC throughout the treatment cycle. Differences between lines A and B increase with DC. At about the mid-point of the DC range tested (DC = 352 mg/L) the effluent alkalinity we observed represents just 15% of that predicted at equilibrium i.e., 87 versus 579 mg/L. Line C shows

Table 3
Effect of AMD source on changes in water chemistry across the test system (*I* = influent mean, *N* = 3; EF = effluent filtered mean, *N* = 3)

Variable	Brandy Camp		Kyler Run	
	I	EF	*I*	EF
pH	4.8 (0.1)	6.2 (0.2)	3.9 (0.1)	6.3 (0.1)
Acidity, mg/L	177.3 (7.6)	64.0 (3.5)	126.7 (10.1)	8.9 (0.9)
Alkalinity, mg/L	5.0 (1.1)	38.0 (6.0)	0.0 (0.0)	51.3 (6.4)
Al, mg/L	5.1 (0.5)	0.2 (0.2)	8.4 (0.9)	0.2 (0.2)
Fe^{2+}, mg/L	54.9 (1.2)	49.5 (2.8)	10.8 (0.3)	9.3 (1.4)
Fe, mg/L	53.0 (3.5)	49.3 (2.7)	11.3 (1.4)	9.4 (0.3)
Mn, mg/L	8.6 (0.5)	7.4 (2.3)	8.2 (0.8)	8.2 (0.2)
Ca, mg/L	126.7 (5.9)	161.3 (2.1)	82.7 (6.0)	116.8 (20.3)

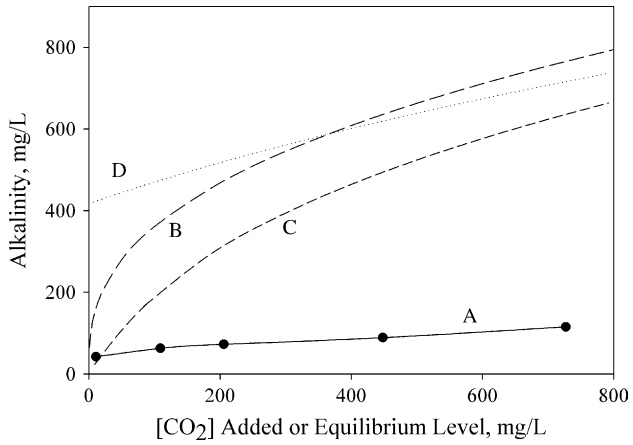

Fig. 4. Comparison of alkalinity observed in Test Series I (line A) with that predicted when the DC concentration is fixed (line B, sulfuric acid acidity = 0 mg/L) and when the DC available is limited to the initial pretreatment concentration (line C, sulfuric acid acidity = 0 mg/L) as well as that generated by acid attack (line D, sulfuric acid acidity = 1000 mg/L).

alkalinity concentrations for the case when CO_2 is limited to that provided by an initial pretreatment charge – without secondary production of CO_2 via Reactions (2) and (3). In this case, line A represents 20% of the 433 mg/L predicted (line C) at the same mid-point DC level (352 mg/L). The difference between alkalinity estimates for cases B and C (146 mg/L) represents the alkalinity increase provided by use of a recirculation loop. Further, differences between alkalinities predicted for case C and our observations (line A) represent unutilized reaction potentials that result from use of a short HRT.

HRT can be increased, when needed, through use of reactors that allow an elevation in settled bed height beyond the 52–53 cm used in our tests. For example, Sibrell et al. (2000) observed a significant increase in alkalinity with increasing PLB bed height (range 30–60 cm), at each of four test operating pressures (0, 34, 82, 118 kPa) as described by the relation: alkalinity (mg/L) = 2.113 (kPa) + 4.38 (cm) − 138, where R^2 = 0.934. A second series of PLB tests with simulated AMD at 140 kPa have been conducted over the bed height range 27.3–77.5 cm (Watten et al., 2004a). In this case alkalinity increased with bed height following the model: alkalinity (mg/L) = $622(1 - e^{-0.0342(cm)})$, where R^2 = 0.881. Both models predict alkalinity will be increased by a factor of about 1.4 as bed height is increased from 30 to 60 cm. Alternatively, Lee (2003) increased HRT by reducing the hydraulic loading rate during the rinse/recharge period of the original PLB process. Effluent alkalinity increased linearly with HRT, e.g., from 300 mg/L at HRT = 6 min to 500 mg/L at 15 min (P_{CO_2} = 34.4 kPa; T = 12 °C). In our tests without intermittent fluidization, however, increasing HRT by reducing hydraulic loading rate did not have a significant effect on effluent alkalinity (Fig. 3). The independence of effluent alkalinity and HRT probably resulted from compensating changes in the active volume of the reactor, as well as the first-order rate constant k_1 that controls the reaction of hydrogen ions with calcite (Eq. (4)). This reaction is considered to be rate limited, at low pH, by the diffusion of reactants to and from reactive surfaces. The constant k_1 is then defined by hydrodynamic conditions and temperature as described by the relation (Sherwood et al., 1975; Sverdrup, 1985):

$$k_1 = \frac{D}{r}\left(1 + 0.3 Re^{1/2} Sc^{1/3}\right) \quad (7)$$

where D is ion diffusivity, and Re and Sc are the Reynold's and Schmidt numbers, respectively, i.e., $Re = V2r/\mu$, $Sc = \mu/D\rho$, μ = kinematic viscosity and ρ = density. Inspection of Eqs. (4) and (7) reveals the reaction of H^+ with calcite is accelerated with increasing turbulence (Re) following the relation $(V)^{0.5}$, e.g., when the effects of hydraulic loading rate were evaluated, in our tests, over the range 571–896 L/m^2/min, upflow velocity increased from 0.95 to 1.49 cm/s and k_1 would be expected to increase by a factor of 1.25 (Eq. (7)). Further compensation for a rising hydraulic loading rate is provided by a linked increase in expanded bed height. This response maintained, in our case, a uniform HRT (1.2 min) within the active or expanded limestone bed zone of the reactor. HRT in a fixed flow application can also be manipulated by changing the radius of the limestone particles. Reducing particle size lowers fluid flux rates required for a target bed expansion ratio (Weber, 1972; Summerfelt and Cleasby, 1993) while increasing the reactive surface area within the bed (Eq. (4)). This response, however, can limit turbulence and interparticle collision forces (Cleasby and Baumann, 1977) needed to avoid excessive scaling of limestone surfaces like that observed by Ghem (1944), Maree et al. (1992) and Maree and du Plessis (1994).

Our tests with alternative timing sequences indicate this variable does not influence effluent alkalinity, at least over the range of conditions tested (Fig. 3). Introducing the feed solution over a relatively short duration does, however, increase the pressure drop across the reactor orifices providing higher levels of energy dissipation/mixing in those cases where armoring or fouling is of concern. For example, the hydraulic loading rate with timing sequences of 10 s/50 s, 20 s/40 s and 30 s/30 s was, respectively, 2238, 1119, and 746 L/m^2/min during the bed expansion phase of the cycle with corresponding mean energy dissipation rates of 271, 68, and 30 w/m^3 (Mott, 1979). Higher hydraulic loading rates also provide a greater degree of bed expansion assisting in the displacement of dislodged solids from the reactor. Intermittent fluidization may retard, however, limestone dissolution in those cases where armoring or fouling of the

limestone surfaces is not of concern. Tests conducted with mine water at each of three DC concentrations showed no significant reduction ($P > 0.05$) of effluent alkalinity with pulsing (Table 1) but comparisons ($N = 5$) based on treatment of acidified well water did show a significant reduction ($P < 0.001$) with pulsing. The reductions observed in this case are probably related to changes in the reactor operating mode (Weber, 1972) from the plug–flow type associated with conventional fluidized sand beds (Rittmann, 1982) to an intermittently operated mixed flow reactor type that no doubt models flow behavior in the PLB reactors. Plug–flow reactors provide superior conversion of reactants to products when reaction rates, like those associated with limestone dissolution (Eq. (4)), increase with reactant concentration (Levenspiel, 1979; Rittmann, 1982).

4.2. Field trials

Table 2 data show effective AMD treatment during short-term runs at the Toby Creek test site (Portal A). The HRT maintained here (7.0–7.4 min) represents a small fraction of that required by alternative fixed bed reactors like the anoxic drain (HRT = 16–192 h, Hedin et al., 1994). Effluent quality improved with CO_2 addition but water was net alkaline with an acceptable pH in both cases evaluated. As expected, the alkalinity established without CO_2 addition (58.7 mg/L) was lower than that reported for a standard PLB reactor (one that included a recycle loop) treating the same AMD source without CO_2 input – 80 mg/L (Watten et al., 2004a). In both PLB configurations, however, the removal of Al and Fe with sample filtering was high and similar, ranging between 97.2–98.6%, and 80.1–85.0%. Removal of Fe^{2+} and Mn^{2+} was also similar but low ranging between 16.2–22.3% and 0–11.2%. The low removal rate of Fe^{2+} and Mn^{2+} is related to the inability of the PLB and other limestone based treatment processes to raise AMD pH above that required for hydrolysis and precipitation of these metals (Evangelou, 1995). This limitation is evident in the Brandy Camp and Kyler Run data summarized in Table 3 as well as PLB data reported for Antrim Mine (Cole et al., 2001a,b), Toby Creek (Sibrell et al., 2000) and Friendship Hill (Sibrell et al., 2003) AMD. When required, complete removal of Fe^{2+} and Mn^{2+} will require a pre- or posttreatment oxidation step based on use of reagents or biochemical reactors like those described by Lovell (1973) and Rose et al. (2003). In pre- versus posttreatment oxidation applications, the acidity generated is neutralized by limestone within the PLB reactors and can therefore reduce the CO_2 feed rate required for a target effluent alkalinity concentration (Watten et al., 2004a). Line D in Fig. 4, for example, gives saturation concentrations of alkalinities predicted for the case when CO_2 is provided by an initial pretreatment charge and by the neutralization of acidity (1000 mg/L) with limestone within the PLB reactors (Reactions (1)–(3)). Acid neutralization here shifts alkalinity well above that predicted for the case where CO_2 is limited to an initial pretreatment charge (line C) – without CO_2 input, line D predicts an equilibrium alkalinity of about 400 mg/L that corresponds to a pretreatment CO_2 charge (line C) of 345 mg/L. The effects of acid neutralization and other important operating conditions on required CO_2 feed rates can be predicted by performing a material balance on CO_2 like that described by Watten et al. (2004a), e.g., dissolved carbon dioxide in the reactor's effluent $[CO_2]_{Effluent}$, is related to the AMD source concentration $[CO_2]_{AMD}$, the carbonator mass transfer rate (M_{CO_2}/L) and the net increase in DC that occurs following acidity (Acy) neutralization and effluent alkalinity (Alk) production (0.44(Acy – Alk)):

$$[CO_2]_{Effluent} = [CO_2]_{AMD} + (M_{CO_2}/L) + 0.44(\text{Acy} - \text{Alk}) \tag{8}$$

Effluent alkalinity, in turn, has been described by the model form $\text{Alk} = a_1 + b_1(\text{DC})^{0.5}$ (Eq. (5)), where a_1 and b_1 are regression coefficients developed for a specific AMD source. Combining this model with Eq. (8), and assuming a mixed liquid phase within the reactor, allows calculation of required carbonator gas feed rates for a target effluent alkalinity:

$$\frac{M_{CO_2}}{L} = \left(\frac{\text{Alk} - a_1}{b_1}\right)^2 - \left(0.44(\text{Acy}) + [CO_2]_{AMD}\right) \tag{9}$$

The ratio M_{CO_2}/L can be reduced, or in some cases eliminated, through transfer of CO_2 from system effluent to system influent (Watten, 1999). Letting E indicate the selected efficiency of the recycle step, as a decimal fraction, results in the following expression for the required carbonator gas transfer rate:

$$\frac{M_{CO_2}}{L} = \left(\frac{\text{Alk} - a_1}{b_1}\right)^2 - \left(E\left(\frac{\text{Alk} - a_1}{b_1}\right)^2 + 0.44(\text{Acy} - \text{Alk}(E)) + [CO_2]_{AMD}\right) \tag{10}$$

Fig. 5, lines A and B show the positive effect of increases in acidity and CO_2 recycling on CO_2 feed requirements as predicted by Eq. (10). In this example, we assume $[CO_2]_{AMD} = 30$ mg/L and that alkalinity yield follows Eq. (5). Note that as acidity increased from 0 to 200 mg/L with $E = 0$, M_{CO_2}/L decreased from 361 to 273 mg/L. The latter was reduced further to lows of 88 and 0 mg/L, respectively, as E approached 0.78. A $[CO_2]_{AMD}$ well above the air saturation concentration is common in AMD (Hedin et al., 1994; Jageman et al., 1988; Pearson et al., 1982), and represents, with

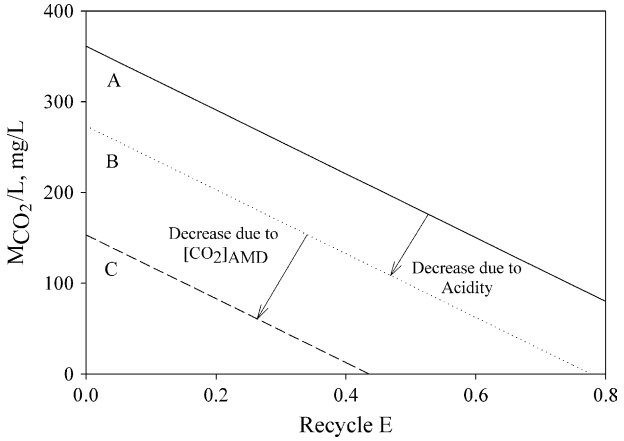

Fig. 5. Model predicted CO_2 feed requirements versus efficiency of CO_2 recovery (E) for the case where inlet acidity = 0 mg/L and $[CO_2]_{AMD}$ = 30 mg/L (line A), inlet acidity = 200 mg/L and inlet $[CO_2]_{AMD}$ = 30 mg/L (line B) and inlet acidity = 200 mg/L and inlet $[CO_2]_{AMD}$ = 150 mg/L (line C).

application of the PLB process, an asset that should be conserved prior to treatment. Jageman et al. (1988), for example, give carbonate concentrations for waters released from three coal mines that show $[CO_2]_{AMD}$ concentrations of about 200, 290 and 340 mg/L. Increasing the $[CO_2]_{AMD}$ in our example (Fig. 5) from 30 mg/L (line B) to 150 mg/L (line C) reduces CO_2 feed requirements in all cases by 120 mg/L and shifts the E value required for $M_{CO_2}/L=0$ from 0.78 to 0.44. CO_2 recovery is accomplished with equipment providing gas–liquid interfacial area within isolated gas transfer chambers including spray towers, packed towers and enclosed surface agitators (Watten, 1999; Sibrell et al., 2000, 2003; Vinci, 2003). The degree of recovery (E) is increased by staging and control of vacuum/pressure within individual stripper and absorber components (Watten, 1999). Selection of the least costly set of operating conditions, including E, will be related to local costs of CO_2, power, reactor capital (amortized) as well as the sensitivity of effluent alkalinity to increases in DC (Eq. (5)).

5. Conclusions

We evaluated a pulsed limestone bed treatment process modified to reduce system complexity so as to broaden the scope of potential applications in the field. Combined, our data demonstrate performance, as measured by limestone dissolution rate, is relatively insensitive to changes in hydraulic loading rate and reactor operating mode such as timing sequence, but can be enhanced by increasing influent DC. The CO_2 feed rate required for a target alkalinity can be reduced or eliminated through conservation of CO_2 present in the AMD and through the recovery and reuse of CO_2 in system effluent. Increases in pH across the system provide for the hydrolysis and removal of Fe^{3+} and Al^{3+}, but not Fe^{2+} and Mn^{2+}. Neutralization of acidity associated with Fe^{+2} and Mn^{2+}, when present, will require a pretreatment step based on use of oxidizing reagents or biochemical reactors. Our short-term tests with AMD acidities of 127 mg/L–340 mg/L showed good treatment without signs of armoring but longer-term trials should be conducted to determine the suitability of the modified process for treatment of a specific AMD source. Alteration of the timing sequence used to fluidized limestone within the reactor provides control of energy dissipation/mixing in those cases where armoring is of concern. The HRT required for treatment (HRT < 10 min) represents a small fraction of the HRT required for alternative fixed beds of coarse limestone like the anoxic drain (HRT > 16 h) providing a potential for savings in costs associated with reactor volume.

Acknowledgement

This project was funded in part by the U.S. Department of Agriculture, Agricultural Research Service (Agreement No. 59-1930-1-130) and the USGS State Partnership Program (No. 1445-CA09-0014).

References

APHA [American Public Health Association, American Water Works Association and Water Environment Federation], 1995. Standard Methods for the Examination of Water and Wastewater, 19th ed. APHA, Washington, DC.

Cleasby, J.H., Baumann, E.R., 1977. Backwash of Granular Filters used in Wastewater Filtration. Rep. No. 600/2-77-016, U.S. EPA, Cincinnati, Ohio.

Cole, M.B., Arnold, D.E., Watten, B.J., 2001a. Physiological and behavioral responses of stonefly nymphs to enhanced limestone treatment of acid mine drainage. Water Res. 35, 625–632.

Cole, M.B., Arnold, D.E., Watten, B.J., Krise, W.F., 2001b. Haematological and physiological responses of brook char to untreated and limestone-neutralized acid mine drainage. J. Fish Biol. 59, 79–91.

Colt, J., 1984. Computation of Dissolved Gas Concentrations in Water as Functions of Temperature, Salinity and Pressure, Special Publication 14. American Fisheries Society, Bethesda, Maryland.

Dempsey, B.A., Jeon, B., 2001. Characteristics of sludge produced from passive treatment of mine drainage. Geochem. Explor. Environ. Anal. 1, 89–94.

EPA, 1983. Methods for Chemical Analysis of Water and Wastes (EPA-600/4-79-020). U.S. Environmental Protection Agency, Cincinnati, Ohio.

Evangelou, V.P., 1995. Pyrite Oxidation and Its Control. CRC Press, Boca Raton, Florida.

Ghem, H.W., 1944. Neutralization of acid waste waters with an up-flow expanded limestone bed. Sewage Work. J. 16, 104–120.

Hammarstrom, J.M., Sibrell, P.L., Belkin, H.E., 2003. Characterization of limestone reacted with acid-mine drainage in a pulsed limestone

bed treatment system at the Friendship Hill National Historical Site, Pennsylvania, USA. Appl. Geochem. 18, 1705–1721.

Hedin, R.J., Watzlaf, G.R., Nairn, R.W., 1994. Passive treatment of coal mine drainage with limestone. J. Environ. Qual. 23, 1338–1345.

Jageman, T.C., Yokley, R.A., Heunisch, G.W., 1988. The use of pre-aeration to reduce the cost of neutralizing acid mine drainage. In: Proceedings of the Fifth Annual Meeting, American Society for Surface Mining and Reclamation Pittsburgh, Pennsylvania, pp. 131–135.

Lee, P.C., 2003. Comparison of two methods for estimating pesticide volatilization from turf, characterizing a pulsed limestone bed reactor to treat high acidity water, and thermal analysis model of zero water exchange indoor shrimp farming systems. Ph.D. dissertation, Cornell University, Ithaca, New York.

Levenspiel, O., 1979. The Chemical Reactor Omnibook. Oregon State University Book Stores Inc., Corvallis, Oregon.

Lovell, H.L., 1973. An appraisal of neutralization processes to treat coal mine drainage. Rep. No. 670/2-73-093, U.S. EPA, Washington, DC.

Maree, J.P., du Plessis, P., van der Walt, C.J., 1992. Treatment of acid effluents with limestone instead of lime. Water Sci. Technol. 26, 345–355.

Maree, J.P., du Plessis, P., 1994. Neutralization of acid mine water with calcium carbonate. Water Sci. Technol. 29, 285–296.

Maree, J.P., van Tonder, G.J., Millard, P., Erasmus, T.C., 1996. Pilot-scale neutralisation of underground mine water. Water Sci. Technol. 34, 141–145.

Mitchell, K.G., Wildeman, T.R., 1996. Solubility of Fe(III) and Al in AMD by modeling and experiment. In: Proceedings of the 13th Annual Meeting American Society for Surface Mining and Reclamation Knoxville, TN, pp. 681–689.

Mott, R.L., 1979. Applied Fluid Mechanics, second ed. Charles E. Merrill Publishing Co., Columbus, Ohio.

Parkhurst, D.L., 1995. User's guide to PHREEQC – A computer program for speciation, reaction-path, advective transport, and inverse geochemical calculation. U.S. Geological Survey – Water Resources Investigations Report 95-4227.

Pearson, F.H., McDonnell, A.J., 1975a. Use of crushed limestone to neutralize acid wastes. J. Environ. Eng. Divis. ASCE 101, 139–158.

Pearson, F.H., McDonnell, A.J., 1975b. Limestone barriers to neutralize acidic streams. J. Environ. Eng. Divis. ASCE 101, 425–440.

Pearson, F., McBride, S., Batcheler, N., 1982. Decarbonation of limestone-treated mine drainage. J. Environ. Eng. Divis. ASCE 108, 957–972.

Plummer, L.N., Wigley, T.M.L., Parkhurst, D.L., 1978. The kinetics of calcite dissolution in CO_2-water systems at 5° to 60 °C and 0.0 to 1.0 ATM CO_2. Am. J. Sci. 278, 179–216.

Rittmann, B.E., 1982. Comparative performance of biofilm reactor types. Biotechnol. Bioeng. 24, 1341–1370.

Rose, A.W., Shah, P.J., Means, B., 2003. Case studies of limestone-bed passive systems for manganese removal from acid mine drainage. In: Proceedings of the 20th Annual Meeting American Society for Mining and Reclamation Billings, Montana, pp. 1059–1078.

Sherwood, T.K., Pigford, R.L., Wilke, C.R., 1975. Mass Transfer. McGraw Hill, Kogakusha, Tokyo.

Sibrell, P.L., Watten, B.J., Boone, T., 2003. Remediation of acid mine drainage at the Friendship Hill National Historic Site with a pulsed limestone bed process. Hydrometallurgy, Vancouver, BC, Canada, pp. 1823–1836.

Sibrell, P.L., Watten, B.J., Friedrich, A.E., Vinci, B.J., 2000. ARD remediation with limestone in a CO_2 pressurized reactor. In: Proceedings of the Fifth International Conference on Acid Rock Drainage, Society for Mining, Metallurgy, and Exploration, Denver, Colorado, pp. 1017–1026.

Sibrell, P.L., Watten, B.J., 2003. Evaluation of sludge produced by limestone neutralization of AMD at the Friendship Hill National Historic Site. In: Proceedings of the 20th Annual Meeting American Society for Mining and Reclamation, Billings, Montana, pp. 1151–1169.

Skousen, J., Politan, K., Hilton, T., Meek, A., 1995. Acid mine drainage treatment systems: Chemicals and costs. In: Skousen, J.G., Ziemkiewicz, P.F. (Eds.), Acid Mine Drainage Control and Treatment. West Virginia University and the National Mine Land Reclamation Center, Morgantown, WV, pp. 121–129.

Starnes, L.B., Gasper, D.C., 1995. Effects of surface mining on aquatic resources in North America. Fisheries 20, 20–23.

Stumm, W., Morgan, J.J., 1996. Aquatic Chemistry. John Wiley & Sons, New York, NY.

Summerfelt, S.T., Cleasby, J.L., 1993. Hydraulics in fluidized-bed biological reactors. Techniques for Modern Aquaculture. ASAE, St. Joseph, Michigan pp. 439–457.

Sverdrup, H.U., 1985. Calcite Dissolution Kinetics and Lake Neutralization. Ph.D. Thesis, Lund Institute of Technology, Lund, Sweden.

Vinci, B.J., 2003. Modeling Treatment of Acid Mine Drainage in a Carbon Dioxide Pressurized Limestone Reactor System. Ph.D. Dissertation. Cornell University, Ithaca, New York.

Watten, B.J., 1999. Process and Apparatus for Carbon Dioxide Pretreatment and Accelerated Limestone Dissolution for Treatment of Acidified Water. U.S. Patent 5914046, U.S. DOC, Washington, DC.

Watten, B.J., Sibrell, P.L., Schwartz, M.F., 2004a. Effect of acidity and elevated P_{CO_2} on acid neutralization within pulsed limestone bed reactors receiving coal mine drainage. J. Environ. Eng. Sci. 21, 786–802.

Watten, B.J., Boyd, C.E., Schwartz, M.F., Summerfelt, S.T., Brazil, B.L., 2004b. Feasibility of measuring dissolved carbon dioxide based on head space partial pressures. Aquacult. Eng. 30, 83–101.

Weber Jr., W.J., 1972. Physicochemical Processes for Water Quality Control. John Wiley & Sons, Inc., New York, NY.

Ziemkiewicz, P.F., Skousen, J.G., Brant, D.L., Sterner, P.L., Lovett, R.J., 1997. Acid mine drainage treatment with armored limestone in open limestone channels. J. Environ. Qual. 26, 1017–1024.

Zurbuch, P.E., 1963. Dissolving limestone from revolving drums in flowing water. Trans. Am. Fish. Soc. 93, 173–178.